NASA TECHNICAL MEMORANDUM

NASA TM X-53344

October 7, 1965

GROUND LEVEL ACOUSTICAL FOCI IN A THREE-LAYERED ATMOSPHERE

by Willi H. Heybey
Aero-Astrodynamics Laboratory

NASA

George C. Marshall Space Flight Center, Huntsville, Alabama

TECHNICAL MEMORANDUM X-53344

GROUND LEVEL ACOUSTICAL FOCI IN A THREE-LAYERED ATMOSPHERE

By

Willi H. Heybey

George C. Marshall Space Flight Center
Huntsville, Alabama

ABSTRACT

14100

An infinitesimally slender bundle of sound rays emitted by a point source can, under certain meteorological conditions, be returned to the horizontal plane on which the source sits, and at the same time, may be narrowed down to enclose an area actually equal to zero. In such cases the common point of arrival is called an acoustical focus. The intensity of returned energy there attains a very high degree capable of damaging effects.

For determining such points the atmosphere is usually divided up into layers in each of which the change of the sound speed with height is considered constant. Three layers often suffice to approximate the many layers arising from observation.

The report studies focus formation engendered by the third layer in collaboration with the two lower layers. A focus may appear in variegated circumstances. For each case a computational scheme is given which may be followed by slide rule or assigned to machines if higher accuracy or a systematic survey is desired.

NASA-GEORGE C. MARSHALL SPACE FLIGHT CENTER

NASA-GEORGE C. MARSHALL SPACE FLIGHT CENTER

TECHNICAL MEMORANDUM X-53344

October 7, 1965

GROUND LEVEL ACOUSTICAL FOCI IN A THREE-LAYERED ATMOSPHERE

By

Willi H. Heybey

AERO-ASTRODYNAMICS

TABLE OF CONTENTS

LIST OF ILLUSTRATIONS

TECHNICAL MEMORANDUM X-53344

GROUND LEVEL ACOUSTICAL FOCI IN A THREE-LAYERED ATMOSPHERE

SUMMARY

The report classifies the states that may occur in a three-layered atmosphere.

For each such class the possible existence of foci is discussed in developing the iterative method for solving the equation valid for foci that evolve from the third layer. Those originating with the second layer are not considered; for these, existence conditions and modes of computation are simple and known.

The location of the focus is given, and the seriousness of the intensity near it is described by a characteristic quantity.

Unexpected features of focus formation are pointed out as, e.g., existence of as many as two third-layer foci in conditions where a similarly structured two-layer atmosphere would support none (even otherwise, it could produce at most one).

Three classes permit a non-iterative, direct solution of the focal equation. They throw in vivid relief some of the novel aspects including the way in which the focal distance and intensity respond to variations of the third-layer velocity gradient.

I. INTRODUCTION

The complex propagation patterns of sound energy in the natural atmosphere become amenable to relatively straightforward mathematical description when three major simplifications are made. First, of all the effects a sound wave may experience, refraction and reflection only are admitted (ray acoustics). Secondly, the propagation velocity of sound is considered a function of height only (stratified atmosphere). An acoustical ray sent out by the point source in a given azimuthal direction then will forever remain in the vertical half-plane

fixed by that direction so that the ray pattern in it can be determined without regard to other such planes. Thirdly, the wind must not have a vertical component (which, incidentally, is hard to measure).

Rothwell (Ref. 1) has dealt with the problem on this basis. The mathematical formulation is still rather involved and the final results are not essentially different from those obtained when two more restrictions of lesser import are made: on the one hand, the wind velocity is assumed as small when compared to the thermodynamic sound speed; on the other, the sound ray inclination should not go above, say, $\theta = 18.5°$ ($\cos\theta = 0.95$). These rays account for the energy return to be expected in the nearer vicinity of the source.

Meteorological observations of temperature, wind velocity, and humidity at specified heights can then be compounded to determine the local velocity of sound prevailing in a selected half-plane. It is customary to connect the discrete data points by straight line segments and thus to break up the stratified atmosphere into plane-bound layers in which the velocity, V, of sound is a linear function of the height (y). In the kth layer it may be written as

$$V = V_{k-1} + \mu_k (y - y_{k-1}) \tag{1}$$

where the index (k-1) refers to the bottom of that planar layer. The coefficient μ_k is evidently given as

$$\mu_k = \frac{V_k - V_{k-1}}{y_k - y_{k-1}} \tag{2}$$

and thus is determined by the top and bottom speeds and the layer's vertical extension. Its numerical value can be positive, zero, or negative, but is never large in practice ($10^{-2}\ \frac{1}{\text{sec}}$ in general). The sound source is placed at the height $y_0 = 0$, so that in the ground layer

$$\mu_1 = \frac{V_1 - V_0}{y_1} \quad .$$

The velocity polygon (customarily height is plotted versus velocity) is different for each vertical half-plane through the source (except in a still

atmosphere). For energy considerations it is necessary to introduce an adjacent half-plane in which the state of the atmosphere is substantially unchanged. The sound field within the infinitesimal vertical wedge formed in this way is conveniently divided into ray tubes originating at the source and widening or narrowing on their courses. Through all the rectangular cross sections of a tube, the same amount of energy is transmitted per time unit because dissipation is not taken into account in ray acoustics. If the cross-sectional area shrinks to zero, as it does when the top and bottom surfaces of the tube gradually approach each other and finally intersect at zero angle, the intensity (energy/ time area) becomes increasingly larger and at the end infinitely large. In the planar representation one then obtains what is called an acoustical focal point.

Infinite intensity will hardly be observed in practice because, for one reason, one cannot measure at a mathematical point; for another, the irregularities of the natural atmosphere tend to dislocate the focus, if not to obliterate exact zero-angle intersections altogether. Also, interference processes might weaken the energy return. However, if ray acoustics indicate a focal point the prima facie assumption appears justified that high sound pressure levels may be expected to occur there.

Evidently a continuous sequence of zero-angle intersections can exist in the open atmosphere forming a spatial point array in the nature of a ray envelope. These focal curves are of special interest in the air space over slightly hilly terrain and will be subject matter of a later memorandum. The present investigation is concerned with their zero-height points only, henceforth called "the" focal points.

The velocity profile as it is obtained from meteorological observation is a many-sided polygon corresponding to a multi-layered atmosphere. The raw material is corrected when necessary (cleaned of doubtful points, etc.) and often smoothed (for a more even data distribution). It may include local effects not characteristic for the atmosphere as a whole, and it is subject to an error margin as any measurement is. The "observed" velocity profile must therefore be envisaged as a more or less accurate approximation to the true vertical velocity distribution.

Since the necessary computer evaluation is numerical, conclusions of a general nature can seldom be made. In freak cases, the result may even be misleading; an instance is known where, with the usual step increase of $\Delta\theta_0 = 0.20$, a focus, known otherwise to be present, was not detected before the step was drastically decreased by the factor 200.

Experience has also shown that ray pattern and focus formation can be surprisingly sensitive to small variations in the meteorological parameters. The first indication of this was given in Reference 2. Reference 3 studies the effect of small data modifications in the two-layer set-up where closed expressions are available eliminating the need for numerical specimen calculations.

The present report undertakes to open the way for similar investigations in the three-layered atmosphere, as far as focus formation is concerned; systematic surveys will be made subsequently. Moreover, a three-sided velocity polygon can frequently be substituted for the many-sided polygon of observation, without stretching the evidence beyond the breaking point. It then may help to show that an observed focus could indeed have been present, although the computer deck did not, and perhaps could not, reveal it. Finally, an insight in characteristic features of focus formation will be provided that goes beyond what is known from the study of the two-layered atmosphere.

II. BACKGROUND AND GENERAL INFORMATION

When ascending rays penetrate into a layer, their upward swing is not being checked unless the velocity gradient, μ, there is positive. If the layer is sufficiently extended in height, the ascent of low inclination rays may be stopped altogether and converted into a downward trend; if so, these rays are sure to hit the ground again. Among them, there might be a focal ray, that is, a ray that at zero level intersects with the adjacent ray under zero angle. Ray inclinations will be identified here by the angle, θ, they make with the local horizontal line. Along the descending portion of the path θ is negative. A ray may be singled out of the mass of all rays by its angle of departure at the source, $\theta = \theta_0$. That of the focal ray will be called θ_0^* .

In order to have a focus out of the third layer, the fundamental requirement must be made that

$$\mu_3 \geqq 0 , \tag{3}$$

which, however, is not the only one. Sufficient conditions will be set up as if the third planar layer extended to unlimited heights, allowing all the rays that enter it to return to ground level. No conceivable focus then can escape attention. After ascertaining that a focus, i.e., a real value of θ_0^* , can exist with a given μ_3, one can determine without difficulty whether or not the focus will in fact appear

if the third layer is terminated at $y = y_3$. The top velocity, V_3, follows from expression (2). Unless

$$\cos \theta_0^* \geqq \frac{V_0}{V_3}, \tag{4}$$

the presumptive focal ray will not be turned around within the third layer and will enter the fourth, so that the focus cannot materialize.

The ground layer can never induce focus formation, but the second (middle) layer can, granted sufficient thickness and a positive velocity gradient. Second layer foci can be dismissed here, since Reference 4 deals with them in considerable detail. The same report also contains the fundamentals of third-layer relations, especially those numbered (55), (57), (58), (59), (p. 40-41). They are given in terms of the quantity

$$\zeta = \cos^2 \theta_0^* \quad .$$

However, it has been found that the mathematical discussion is facilitated if, instead of ζ, the cotg - function is used:

$$q = \operatorname{cotg}^2 \theta_0^* \tag{5}$$

Equation (55) of Reference 4 contains a misprint (the factor K_2^2 in the third square root should be K_1^2); after correction is made, it assumes the form

$$1 - \frac{D_2}{\sqrt{1 + \delta_1 q}} + \frac{D_2 - D_3}{\sqrt{1 + \delta_2 q}} = 0 \tag{6}$$

where

$$\left.\begin{aligned} D_i &= 1 - \frac{\mu_1}{\mu_i} \\ \delta_i &= 1 - K_i^2 \\ K_i &= \frac{V_i}{V_0} \quad . \end{aligned}\right\} \tag{6a}$$

If a real and positive solution q exists to equation (6), the third layer induces a focal point, the focal ray departing at the source with the elevation $\theta_0^* = \text{arc cotg } \sqrt{q}$. This ray impinges on the horizontal plane at a distance, x_F, from the source given by expression (57), now written as

$$x_F = \frac{2y_1}{K_1 - 1} \frac{1}{\sqrt{q}} \left[1 - D_2 \sqrt{1 + \delta_1 q} + (D_2 - D_3) \sqrt{1 + \delta_2 q} \right]. \quad (7a)$$

It is sometimes convenient to use a second representation of x_F obtainable by combining relations (6) and (7a) to give

$$x_F = \frac{2y_1}{K_1 - 1} \sqrt{q} \left[\frac{-D_2 \delta_1}{\sqrt{1 + \delta_1 q}} + \frac{(D_2 - D_3) \delta_2}{\sqrt{1 + \delta_2 q}} \right] . \quad (7b)$$

A measure of how strongly the intensity becomes infinite at the focus is provided by the quantity, ω, which is proportional to the intensity average in a differential vicinity of the focus; relation (58) of Reference 4 is transformed into

$$\omega = \frac{4\sqrt{q}}{x_F \left. \frac{d^2 x_S}{d\theta_0^2} \right|_{\theta_0 = \theta_0^*}} \quad (8)$$

where, by expression (59),

$$\left. \frac{d^2 x_S}{d\theta_0^2} \right|_{\theta_0 = \theta_0^*} = \frac{2y_1}{K_1 - 1} \frac{(1 + q)^2}{\sqrt{q}} \left[\frac{-D_2 \delta_1}{(1 + \delta_1 q)^{3/2}} + \frac{(D_2 - D_3) \delta_2}{(1 + \delta_2 q)^{3/2}} \right] . \quad (9)$$

Formulas (7b), (8), (9) indicate that ω is mainly determined by the ratio $\frac{\sqrt{q}}{(1 + q)^2}$. Before θ_0^* waxes larger than permissible, the severity of a focal situation will in general increase as θ_0^* increases; larger elevation

focal rays threaten higher sound pressure levels. There are exceptions to this rule, as will be seen in Section VII. The focal point generally will move toward the sound source if θ_0^* is increased.

III. ON COMPUTING SOURCE LEVEL FOCI EVOLVING FROM THIRD-LAYER CONDITIONS

In Figure 1 some forms of the three-sided velocity polygon are sketched (many more of them must be distinguished). The slope, $\tan(\frac{\pi}{2} - \arctan \mu_k)$,

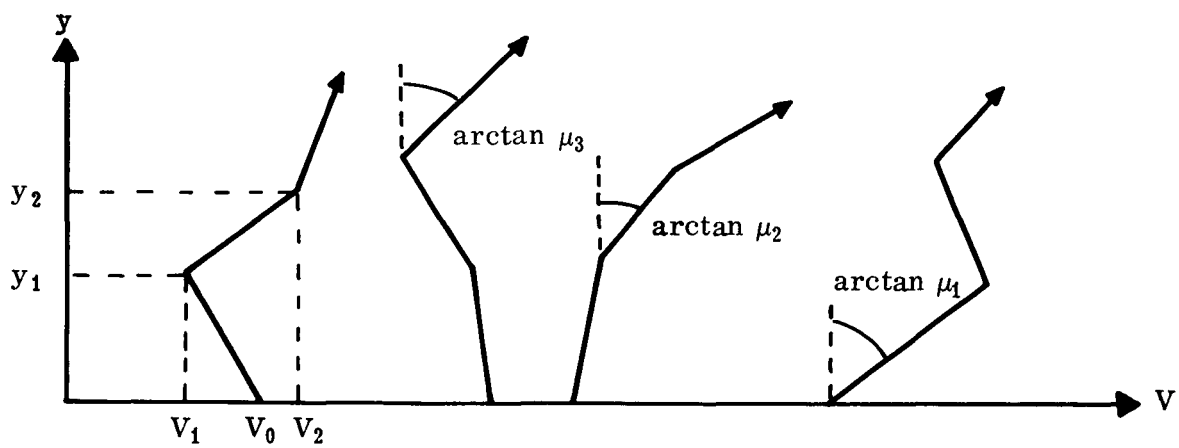

FIGURE 1. SOME FORMS OF THREE-LAYER VELOCITY PROFILES

of the kth side is positive, infinite, or negative depending on whether μ_k is positive, zero, or negative. By condition (3) that of the uppermost side must not be negative. Otherwise, the polygons can have any shape as the choice of V_0, V_1, V_2, y_1, y_2 is completely free, at least mathematically. In physical reality, the three velocities will not differ very much from each other so that by definition (2), the μ_k as a rule will be small quantities. Likewise, the $\delta_k = 1 - \left(\frac{V_k}{V_0}\right)^2$ will be small.

It is seen that the quantities δ_1 and δ_2 can be chosen independently from each other, and also from both D_2 and D_3:

$$D_2 = 1 - \frac{\mu_1}{\mu_2} = 1 - \frac{V_1 - V_0}{V_2 - V_1} \quad \frac{y_2 - y_1}{y_1}$$

$$D_3 = 1 - \frac{\mu_1}{\mu_3} = 1 - \frac{V_1 - V_0}{y_1} \quad \frac{1}{\mu_3} \quad .$$

Note that μ_3 cannot be replaced here by $\frac{V_3 - V_2}{y_3 - y_2}$, since the third layer has been taken as infinitely extended; the physical impossibility of this cannot prevent us from ascribing a value to μ_3. This quantity must be taken as a parameter independent of the five cited above.

Since the focal equation (6) contains four independent parameters, the general discussion of possible roots $q \geqq 0$ offers great difficulties. It was decided not to remove the irrationalities by two times squaring: First, the resulting rational equation is of fourth degree so that the roots depend in a complex manner on the coefficients; second, the coefficients in themselves are unwieldy power combinations of $\delta_1, \delta_2, D_2, (D_2 - D_3)$, all but preventing an elementary classification of the solutions; third, the roots would have to be checked back with the original equation because some of them will not solve it. *

If one stays with the original equation, the convergence criterion of Newton's approximation often requires here that the root sought should already be almost exactly known. By contrast, the convergence requirements when solving iteratively proved to be less stringent.

In order that a process

$$x_{\nu+1} = f(x_\nu)$$

should converge, it is necessary and sufficient that the root and all the iterated

---

* Graeffe's numerical method has been successfully programmed for the fourth degree equation by Mr. Q. Peasley. It gives the four roots with great accuracy, unless two of them have equal modulus, when the deck is not applicable.

values leading to it stay in an x-interval where

$$\left|\frac{df}{dx_\nu}\right| < 1 .$$

If one attempts to satisfy this condition, easier criteria are obtained when the convergence is monotonic rather than oscillatory. To insure this, the derivative must not be negative within the interval. Depending on the signs of the coefficients one will set the equation (6) into several iterative forms such that, if convergence takes place, it is monotonic. In this context it should be noted that the quantities

$$u = \sqrt{1 + \delta_1 q}, \quad v = \sqrt{1 + \delta_2 q}, \quad r = \frac{1}{u}, \quad s = \frac{1}{v} \tag{10}$$

are all not negative for a physical reason. The ascending focal ray leaving the source at the positive (or zero) angle θ_0^* will enter the second and third layers at positive angles, θ_1^* and θ_2^*. Physically, the square roots u and v are the ratios

$$\frac{\sin \theta_0^*}{\sin \theta_1^*}, \quad \frac{\sin \theta_0^*}{\sin \theta_2^*}$$

and therefore not negative. This happy circumstance lessens the variety of forms equation (6) must be given and is otherwise of help in solving it. Since we wish to stay away from squaring the equation, one of the four quantities (10) will have to be taken as the unknown variable. From the outset then, the interval in which to investigate the derivative is restricted to values of the argument that are not negative.

Four basic forms emerge on arranging equation (6) for iterative purposes:

$$r = \frac{1}{D_2}\left[1 + \frac{(D_2 - D_3)\, r}{\sqrt{(1 - \frac{\delta_2}{\delta_1})\, r^2 + \frac{\delta_2}{\delta_1}}}\right] = f(r) \tag{11}$$

$$\frac{df}{dr} = \frac{\frac{\delta_2}{\delta_1}\ \frac{D_2 - D_3}{D_2}}{\left[\left(1 - \frac{\delta_2}{\delta_1}\right) r^2 + \frac{\delta_2}{\delta_1}\right]^{3/2}}$$

$$s = \frac{1}{D_2 - D_3}\left[\frac{D_2 s}{\sqrt{\left(1 - \frac{\delta_1}{\delta_2}\right) s^2 + \frac{\delta_1}{\delta_2}}} - 1\right] = f(s) \qquad (12)$$

$$\frac{df}{ds} = \frac{\frac{\delta_1}{\delta_2}\ \frac{D_2}{D_2 - D_3}}{\left[\left(1 - \frac{\delta_1}{\delta_2}\right) s^2 + \frac{\delta_1}{\delta_2}\right]^{3/2}}$$

$$u = D_2 - \frac{(D_2 - D_3)\, u}{\sqrt{\left(1 - \frac{\delta_2}{\delta_1}\right) + \frac{\delta_2}{\delta_1} u^2}} = f(u) \qquad (13)$$

$$\frac{df}{du} = \frac{-(D_2 - D_3)\left(1 - \frac{\delta_2}{\delta_1}\right)}{\left[\left(1 - \frac{\delta_2}{\delta_1}\right) + \frac{\delta_2}{\delta_1} u^2\right]^{3/2}}$$

$$v = -(D_2 - D_3) + \frac{D_2 v}{\sqrt{\left(1 - \frac{\delta_1}{\delta_2}\right) + \frac{\delta_1}{\delta_2} v^2}} = f(v) \qquad (14)$$

$$\frac{df}{dv} = \frac{D_2\left(1 - \frac{\delta_1}{\delta_2}\right)}{\left[\left(1 - \frac{\delta_1}{\delta_2}\right) + \frac{\delta_1}{\delta_2} v^2\right]^{3/2}} \quad .$$

Many alternative representations can be tried, of which one was found to be more useful in certain circumstances than any of the basic forms:

$$v = \sqrt{\frac{1 - \frac{\delta_1}{\delta_2}}{\left(\frac{D_2}{v + D_2 - D_3}\right)^2 - \frac{\delta_1}{\delta_2}}} = g(v) \qquad (15)$$

$$\frac{dg}{dv} = \frac{D_2^2 \sqrt{1 - \frac{\delta_1}{\delta_2}}}{\left[D_2^2 - \frac{\delta_1}{\delta_2} (v + D_2 - D_3)^2\right]^{3/2}}$$

The roots in these expressions are all not negative, so that the sign of the derivatives solely depends on those of the parameter combinations in front of the roots. Even if these are not negative, the derivative, in addition, must remain smaller than unity to insure monotonic convergence. The r- and s- approaches are both necessary for this reason, although they have non-negative derivatives for the same values of $\frac{\delta_2}{\delta_1}$, D_2, $(D_2 - D_3)$.

For determining the range of applicability of the several representations the quantity

$$D_2 = 1 - \frac{\mu_1}{\mu_2}$$

has been proved a fitting guide. It can vary from $-\infty$ ($\mu_1 > 0$, $\mu_2 = 0$) to $+\infty$ ($\mu_1 < 0$, $\mu_2 = 0$). This vast interval can be split into subintervals marked off by certain values of D_2 for which equation (6) assumes special forms to be treated separately in later sections. Among these values are $D_2 = \pm \infty$ (zero velocity gradient in the second layer), $D_2 = 0$ (equal gradients in the two lower layers), $D_2 = 1$ (zero gradient in the first layer; $\delta_1 = 0$). To these will be added the value of D_2 corresponding to $\delta_2 = 0$ since this clearly is an exceptional case, too. $K_2 = 1$ here, so that, from the definition (2)

$$\frac{\mu_1}{\mu_2} = \frac{K_1 - 1}{K_2 - K_1} \quad \frac{y_2 - y_1}{y_1} = 1 - \frac{y_2}{y_1}$$

$$D_2 = \frac{y_2}{y_1} \quad .$$

This value of D_2 is larger than unity.

Four subdomains emerge in that way:

A. $-\infty < D_2 < 0$ corresponding to $+\infty > \frac{\mu_1}{\mu_2} > 1$

B. $0 < D_2 < 1$ corresponding to $1 > \frac{\mu_1}{\mu_2} > 0$

C. $1 < D_2 < \frac{y_2}{y_1}$ corresponding to $0 > \frac{\mu_1}{\mu_2} > 1 - \frac{y_2}{y_1}$

D. $\frac{y_2}{y_1} < D_2 < +\infty$ corresponding to $1 - \frac{y_2}{y_1} > \frac{\mu_1}{\mu_2} > -\infty$

In each of these subdomains the difference

$$(D_2 - D_3) = -\frac{\mu_1}{\mu_2} \left(1 - \frac{\mu_2}{\mu_3}\right) \tag{16}$$

can have both signs depending on whether $\mu_3 > \mu_2$ or $\mu_3 < \mu_2$. (The case $\mu_3 = \mu_2$ is trivial since the atmosphere becomes two-layered.)

It has been found that in a given subdomain the same iterative representations can be used to arrive at solutions for q and thus for θ_0^*. A single one always suffices when the (non-negative) gradient in the top layer is larger than that in the layer below it. One may recall that, in a two-layered atmosphere, ground foci can exist on this condition only. It will be shown in Section V that with three layers, the condition can be violated without completely eliminating focus formation. On the contrary, as an additional novel feature, even two focal points may appear in some subdomains of D_2, so that two different iterative processes will have to be used in these.

IV. VELOCITY POLYGONS WITH $\mu_3 > \mu_2$

The gradient μ_3 must obey the condition (3); μ_2 and μ_1 should not be equal or zero, nor V_2 equal to V_0, since otherwise equation (6) would assume special forms not covered by the representations (11) to (15).

As an example, the class C will be treated in some detail. Since $\frac{\mu_2}{\mu_1} < -\frac{y_1}{y_2 - y_1}$ in that class, the ratio

$$\frac{\delta_2}{\delta_1} = \frac{K_2 + 1}{K_1 + 1} \left[1 + \frac{\mu_2}{\mu_1} \frac{y_2 - y_1}{y_1} \right] \tag{17}$$

is negative in it, $\frac{\delta_2}{\delta_1} < 0$. Bearing this in mind and applying the approach (15) we derive from the convergence criterion $g'(v_\nu) < 1$, that any iterated value, v_ν, must satisfy the inequality

$$(v_\nu + D_2 - D_3)^2 > -\frac{\delta_2}{\delta_1} D_2^2 \frac{1 - Q}{Q} = (1 - \frac{\delta_2}{\delta_1}) Q^2 (1 - Q) \tag{18}$$

where Q^3 is defined as

$$Q^3 = \frac{D_2^2}{1 - \frac{\delta_1}{\delta_2}} \tag{19}$$

If all the v_ν do so, the convergence is ensured and will be monotonic since, with the approach (15), $\frac{dg}{dv_\nu}$ is always positive.

If the positive quantity Q is at least equal to unity, the criterion (18) is satisfied with any v_ν. However, when

$$0 < Q < 1$$

we must specifically make sure that all the iterated values (including the final one considered as the solution) reside in the convergence interval (18). Suppose the νth iterated value does so. The $(\nu + 1)^{th}$ one,

$$v_{\nu+1} = \sqrt{\frac{1 - \frac{\delta_1}{\delta_2}}{\left(\frac{D_2}{v_\nu + D_2 - D_3}\right)^2 - \frac{\delta_1}{\delta_2}}}$$

then has a lower bound

$$v_{\nu+1} > \sqrt{(1 - \frac{\delta_2}{\delta_1})\ (1 - Q)}$$

which, to secure convergence, ought to be at least equal to the bound imposed by the criterion (18):

$$\sqrt{(1 - \frac{\delta_2}{\delta_1})\ (1 - Q)} \geqq -(D_2 - D_3) + Q\sqrt{(1 - \frac{\delta_2}{\delta_1})\ (1 - Q)} \quad .$$

By expression (16) the difference $(D_2 - D_3)$ is positive in the subdomain C as long as we keep to the assumption that $\mu_3 > \mu_2$. With Q being smaller than unity, the above condition is then satisfied. It would not necessarily be so in a case where $\mu_3 < \mu_2$ which therefore calls for a different iterative approach.

It remains to determine an appropriate initial value, v_1, to start the process when $Q < 1$. For this purpose we may consider the function

$$G(v) = g(v) - v$$

which will be zero for the desired solution or solutions of equation (15). The curve G(v) has a point of inflection at $v = \tilde{v} = -(D_2 - D_3) < 0$ and a maximum at

$$v = v^* = -(D_2 - D_3) + Q\sqrt{(1 - \frac{\delta_2}{\delta_1})\ (1 - Q)}$$

which, however, does not exist with $Q \geqq 1$. Typical forms are shown in Figure 2.

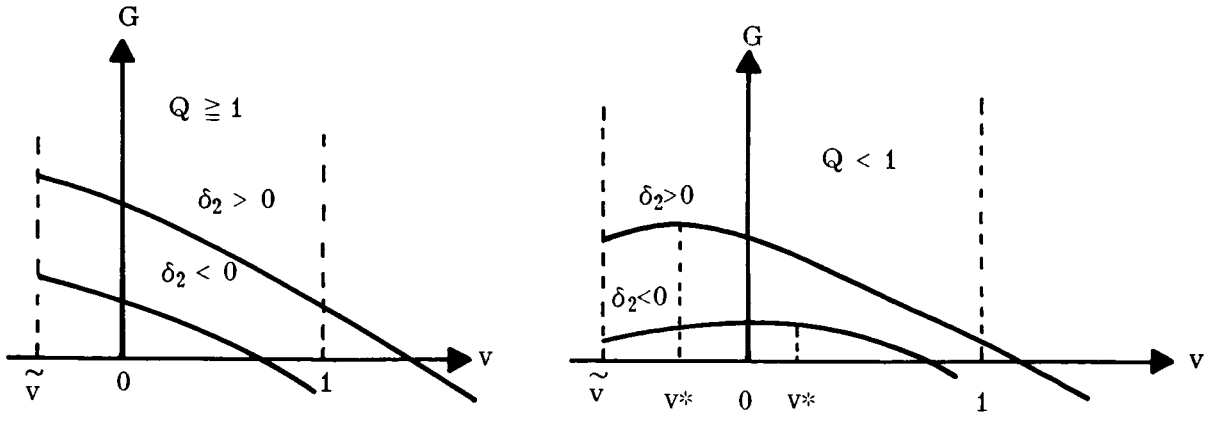

FIGURE 2. PLOTS OF THE FUNCTION G VERSUS ITS ARGUMENT

Since in the subdomain C

$$D_2^2 \left(1 - \frac{\delta_1}{\delta_2}\right)^2 > 1$$

it follows from the definition (19) that

$$Q \left(1 - \frac{\delta_1}{\delta_2}\right) > 1 \qquad (20)$$

and that, therefore, as $Q < 1$,

$$\left(1 - \frac{\delta_2}{\delta_1}\right) (1 - Q) < 1.$$

As a consequence, $v^* < 1$. The convergence condition (18) can be written as

$$v_\nu > v^*$$

from which relation it appears that a suitable first value could be taken as

$$v_1 = 1 .$$

With $Q \geqq 1$ the same value will do (as, indeed, any other would).

Figure 2 indicates, in addition, that in all circumstances there will be one, and only one, point at which G is zero with a positive value of v. (It is easy to back this up by direct analysis of the function G). Thus, in a three-layered atmosphere where $\mu_3 > \mu_2$ and D_2 is located in the subdomain C there is always a single focal ray setting out at the source under an angle θ_0^* given by

$$\operatorname{cotg} \theta_0^* = \sqrt{\frac{1 - v^2}{K_2^2 - 1}}$$

where v is found by the iterative process (15). Its point of impact is determined by expressions (7a) or (7b).

Similar derivations can be made with D_2 chosen in the three other subdomains. To summarize: In subdomain

A. use s-approach and $s_1 = \dfrac{1}{1 - \dfrac{\delta_1}{\delta_2}} \quad \dfrac{D_2}{D_2 - D_3}$

B. use approach (14) and $v_1 = 1 + \dfrac{D_3 - 1}{1 - D_2 \left(1 - \dfrac{\delta_1}{\delta_2}\right)}$

C. use approach (15) and $v_1 = 1$

D. use r-approach and $r_1 = \dfrac{1}{1 - \dfrac{\delta_2}{\delta_1}} \quad \dfrac{D_2 - D_3}{D_2}$.

In all these atmospheric conditions a single zero level focus will exist rooted in the (unlimited) third layer. The eight types of velocity profiles involved are shown in Figure 3; care has been taken to depict $\mu_2 \neq \mu_1$, $\mu_2 \neq 0$, $\mu_1 \neq 0$, $V_2 \neq V_0$.

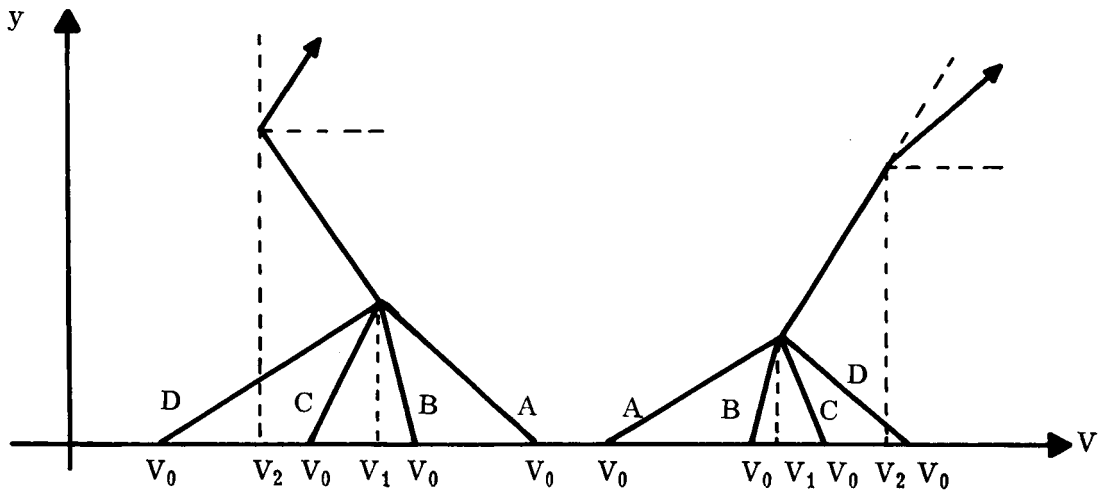

FIGURE 3. TYPES OF VELOCITY PROFILES WITH $\mu_3 > \mu_2$

V. VELOCITY PROFILES WITH $0 \leqq \mu_3 < \mu_2$

There is no chance here that μ_2 could be zero or μ_3 negative, but the other exemptions listed at the beginning of the preceding section apply also.

The subdomain C where

$$\frac{\mu_1}{\mu_2} < 0, \quad \frac{\delta_2}{\delta_1} < 0$$

may again be chosen as a model. Statements more definite than before can now be made. Since the second layer gradient μ_2 is positive, μ_1 will be negative with the further consequences that $V_1 < V_0$, $K_1 < 1$, $\delta_1 > 0$, $\delta_2 < 0$, $K_2 > 1$, $V_2 > V_0$. The polygon C in the later Figure 5 reflects these results.

Expression (16) shows that $(D_2 - D_3)$ is now negative, while D_2 is positive in subdomain C. All of the processes (11) to (15) would converge monotonically. If we select the u-approach (13), $u = \sqrt{1 + \delta_1 q}$ will be larger than unity, and u^2 must be smaller than $(1 - \frac{\delta_1}{\delta_2})$, since otherwise the function

$$F(u) = f(u) - u = (D_2 - u) - \frac{(D_2 - D_3)\, u}{\sqrt{(1 - \frac{\delta_2}{\delta_1}) + \frac{\delta_2}{\delta_1} u^2}} \quad . \quad (21)$$

would not be real. If a focus is to exist, a physically relevant solution of the equation F = 0 must be sought in the interval

$$1 < u < \sqrt{1 - \frac{\delta_1}{\delta_2}} \quad . \quad (22)$$

Aside from the quantity (19), Q^3, it is useful here to consider a further positive combination, **R**, defined by

$$R^3 = \frac{(D_2 - D_3)^2}{1 - \frac{\delta_2}{\delta_1}} \quad . \quad (23)$$

The convergence criterion, $f'(u_\nu) < 1$, then requires that

$$u_\nu < \sqrt{(1 - \frac{\delta_1}{\delta_2})\ (1 - R)} \quad . \quad (24)$$

If u_ν obeys that condition, the next iterated value

$$u_{\nu+1} = D_2 - \frac{(D_2 - D_3)\, u_\nu}{\sqrt{(1 - \frac{\delta_2}{\delta_1}) + \frac{\delta_2}{\delta_1} u_\nu^{\,2}}}$$

is subject to an upper bound

$$u_{\nu+1} < D_2 + R \sqrt{(1 - \frac{\delta_1}{\delta_2})\ (1 - R)}$$

which, to secure convergence, must not be larger than the right side in the criterion (24). On substituting Q for D_2 this gives the condition

$$Q + R \leqq 1 \tag{25}$$

which must be satisfied by the given values of $\frac{\delta_2}{\delta_1}$, D_2, $(D_2 - D_3)$. Convergence here does not take place in all circumstances as it did, regarding v, in Section IV.

Condition (25) has both physical and geometric connotations.

As to the first, we note that the physical inequality (22) must be expected to hold as well at least for iterated values u_ν close to the one that is taken as the root u. Now, Q and R, being positive, are true fractions according to condition (25), so that, by the convergence criterion (24), $u_\nu < \sqrt{1 - \frac{\delta_1}{\delta_2}}$, as it is required. Moreover, condition (25) gives

$$(1 - R)\ (1 - \frac{\delta_1}{\delta_2}) \geqq Q\ (1 - \frac{\delta_1}{\delta_2}) \ .$$

Since relation (20) is valid in the subdomain C, the right side here is larger than unity. Were it otherwise, the left member of the continued inequality (22) could not be satisfied with any u_ν because of condition (24).

Geometrically, analysis of the function F(u) shows that the curve F can have forms as depicted in Figure 4. There is a minimum at

$$u^* = \sqrt{(1 - \frac{\delta_1}{\delta_2})\ (1 - R)} \ .$$

The value $F(u^*)$ is positive, zero, or negative depending on whether $Q + R \gtreqless 1$. It is seen that, if the criterion (25) is satisfied, there exist in general two relevant roots u of the equation $F(u) = 0$, except with the sign of equality when there is only one. If $Q + R > 1$, positive roots cannot exist, and focal points will not originate in the third layer. It is remarkable that the existence condition for foci also insures the convergence of the iterative u-process. However, the latter gives only one of the roots. Since the convergence criterion (24) may be written as

$$u_\nu < u^*$$

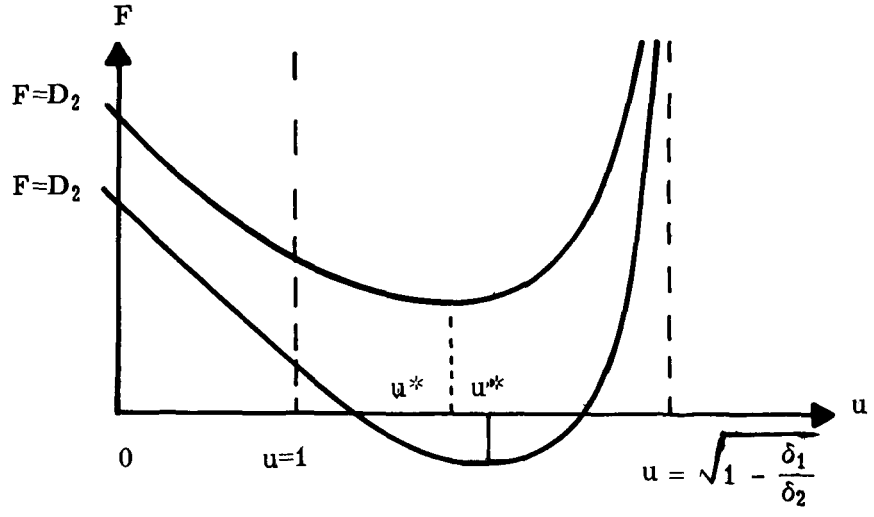

FIGURE 4. GEOMETRY OF THE FUNCTION F(u)

this is the one at the left of the minimum abscissa. A suitable starting value for the iteration will be the abscissa, $u = u_1$, at which the tangent to the curve at $u = 1$ intersects with the u-axis:

$$u_1 = 1 + \frac{D_3 - 1}{1 + (D_2 - D_3)\left(1 - \frac{\delta_2}{\delta_1}\right)} \tag{26}$$

Looking for the second root we may try the s-approach (12) where the convergence criterion, $f'(s_\nu) < 1$, takes the form

$$s_\nu^2 > \frac{1}{R} \frac{Q + R}{1 - \frac{\delta_2}{\delta_1}} \tag{27}$$

It can be shown that all the iterated values remain in this interval if, again, condition (25) is satisfied. This remains true, even when the criterion (27) is made stronger by demanding that

$$s_\nu^2 > \frac{1}{R\,(1 - \frac{\delta_2}{\delta_1})}$$

or that

$$1 + \delta_2 q_\nu < R(1 - \frac{\delta_2}{\delta_1})$$

$$1 + \delta_1 q_\nu = u_\nu^2 > (1 - \frac{\delta_1}{\delta_2})\,(1 - R) = (u^*)^2 .$$

Thus, the s-approach yields the desired value of q corresponding to the root of $F(u) = 0$ at the right of the abscissa u^*. A suitable first value, $s = s_1$, is given in the list below.

The u- and s-approaches converge monotonically, under the conditions stated, not only in C, but also in the subdomain B where, however, $\frac{\delta_2}{\delta_1} > 1$, and therefore $R < 0$.

The study of the velocity profiles with $0 \leqq \mu_3 < \mu_2$ uncovers a less uniform picture of focal possibilities than was found with $\mu_3 > \mu_2$. A survey follows.

Subdomain A. ($D_2 \leqq 0$): No ground level foci originate in the third layer.

Subdomains B. and C. ($0 < D_2 < \frac{y_2}{y_1}$, excepting $D_2 = 1$).

There is no focus in B, if $Q + R < 1$

There is no focus in C, if $Q + R > 1$

There is one single focus if $Q + R = 1$

There are two foci in B, if $Q + R > 1$

There are two foci in C, if $Q + R < 1$

These two can be determined by employing the u- and s-iterations and the initial values

$$u_1 = 1 + \frac{D_3 - 1}{1 + (D_2 - D_3)\left(1 - \frac{\delta_2}{\delta_1}\right)}$$

$$s_1 = \frac{1}{D_2 - D_3}\left(\frac{D_2}{\sqrt{1 - \frac{\delta_1}{\delta_2}}} - 1\right) .$$

If $Q + R = 1$, a direct solution without iteration can be given:

$$\operatorname{cotg}^2 \theta_0^* = \frac{\left[D_2\left(1 - \frac{\delta_1}{\delta_2}\right)\right]^{2/3} - 1}{\delta_1} .$$

Subdomain D. $\left(D_2 > \frac{y_2}{y_1}\right)$. There is always one, and only one, focus originating in the third layer. Use u-approach and

$$u_1 = D_2 - \sqrt{\frac{\delta_1}{\delta_2}}\,(D_2 - D_3) .$$

Figure 5 sketches the four types of profiles involved. The type A where the polygon sides consistently turn to the left produces no ground layer focus, either from the third or from the second layer, although the velocity gradients are positive so that all the rays emitted return to the source horizontal. Note also that if $D_2 > \frac{y_2}{y_1}$ (subdomain D) there will always exist one single zero level focus from the unlimited third layer, regardless of all other meteorological data, especially of whether $\mu_3 < \mu_2$ or $\mu_3 > \mu_2$ (Fig. 3), -as long as μ_3, of course, is not negative.

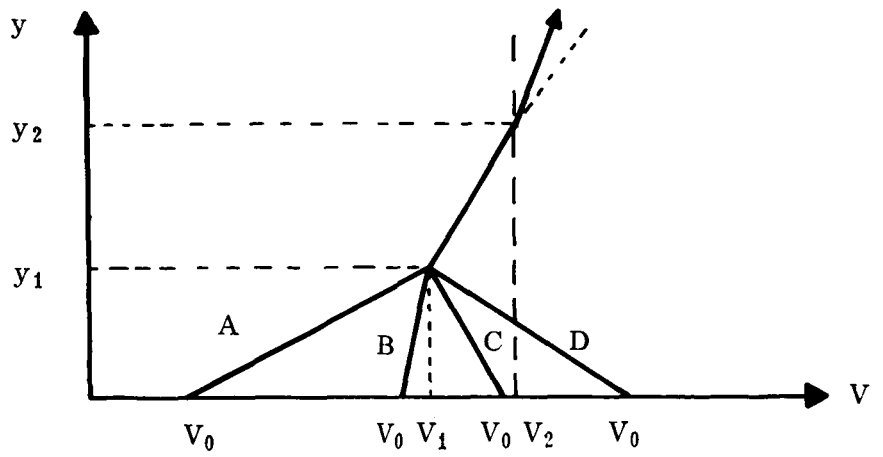

FIGURE 5. THREE-LAYER VELOCITY PROFILES WHEN $0 \leqq \mu_3 < \mu_2$

VI. THREE SPECIAL TYPES OF VELOCITY PROFILES

The focal equation (6) for determining θ_0^* assumes different analytic forms with those values of D_2 that separate the four subdomains A, B, C, D. With $D_2 = \pm\infty$ and $D_2 = 1$ a limiting process is called for; with $D_2 = 0$ and $D_2 = \frac{y_2}{y_1}$ equation (6) affords simple solutions without the need for iteration. The fourth case ($D_2 = \frac{y_2}{y_1}$, $V_2 = V_0$) is especially instructive, since it comprises three fairly general classes of three-sided polygons that can be treated systematically without numerical effort (Section VII).

The iteration procedures recommended in the following can be substantiated by analyses after the pattern set forth in discussing the subdomain C. Special turns have to be added in places. However, as in the preceding sections, leaving small conceptual laps open seemed preferable to developing the main guiding ideas by often lengthy (and rather elementary) mathematical reasoning.

A. $D_2 = \pm \infty$

The gradient in the second layer here is $\mu_2 = 0$, so that $V_2 = V_1$ and $\delta_2 = \delta_1$. The profiles associated with these data fall into the two categories indicated in Figure 6. The case $\mu_1 = 0$ adduces a two-layer situation and is ex-

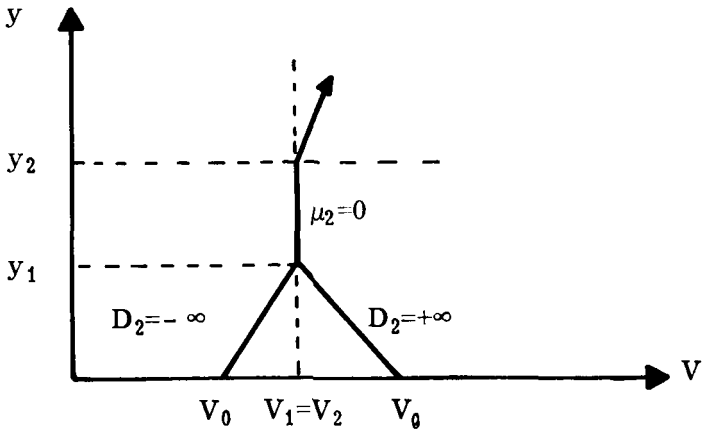

FIGURE 6. PROFILES WITH $\mu_2 = 0$

cluded for that reason. Since both D_2 and δ_2 contain aggregates in K_2 and K_1, one performs the necessary limiting process by letting K_2 approach K_1. Equation (6) then assumes the form

$$u^3 = \beta + (D_3 - \beta)u^2 \tag{28}$$

where

$$\beta = \frac{K_1}{K_1 + 1} \quad \frac{y_2 - y_1}{y_1} \quad . \tag{29}$$

For iterative treatment one best introduces the unknown

$$w = u^3 = (1 + \delta_1 q)^{3/2} , \tag{30}$$

so that

$$w_{\nu+1} = \beta + (D_3 - \beta)\, w_{\nu}^{2/3} = h(w_{\nu}) \,. \tag{31}$$

Since $\frac{dh}{dw_{\nu}}$ is positive with $(D_3 - \beta)$, the approach (31) will be used only when $(D_3 - \beta) > 0$. An initial value has been determined as

$$w_1 = (D_3 - \beta)^3 + 3\beta \,.$$

The very special case $(D_3 - \beta) = 0$ gives the direct solution

$$\operatorname{cotg}^2 \theta_0^* \doteq \frac{1}{\delta_1} \quad (\beta^{2/3} - 1) \,.$$

Note that here $\beta(= 1 - \frac{\mu_1}{\mu_2})$ is smaller than unity if $\delta_1 < 0$ $(\mu_1 > 0)$, and vice versa.

With $(D_3 - \beta) < 0$ the reciprocal $\rho = \frac{1}{w}$ leads to the monotonically converging process

$$\rho_{\nu+1} = \frac{1}{\beta} \left[1 + (\beta - D_3)\, \rho_{\nu}^{1/3} \right] \tag{32}$$

where

$$\rho_1 = \frac{2}{3\beta} + \left(\frac{\beta - D_3}{\beta} \right)^{3/2}$$

is a suitable starting value.

In all circumstances one (and only one) source level focus will be produced by the third layer. The situation is similar to that depicted by the left diagram of Figure 3.

The limiting process $K_2 \to K_1$ if applied to the expressions (7b) and (8) yield formulas that can be further rearranged by the use of the focal equation

(28). The final results may be written as

$$x_F = 2y_1 (K_1 + 1) \sqrt{\frac{q}{1 + \delta_1 q}} \quad (2\beta + \sqrt{1 + \delta_1 q})$$

$$\omega = \frac{1}{\left[(K_1 + 1) y_1\right]^2} \frac{\sqrt{q}}{(1 + q)^2} \quad \frac{(1 + \delta_1 q)^3}{\left[2\beta + \sqrt{1 + \delta_1 q}\right]\left[2\beta + (1 + \delta_1 q)^{3/2}\right]} .$$

B. $D_2 = 0$

This in fact is a two-layer case, as $\mu_2 = \mu_1$. Equation (6) is easily solved:

$$\sqrt{1 + \delta_2 q} = D_3 \; ; \quad q = \operatorname{cotg}^2 \theta_0^* = \frac{D_3^2 - 1}{1 - K_2^2} \quad .$$

The solution is real if the gradient in the third layer (μ_3) is not negative and at the same time larger than the gradient in the layer below it (μ_2).* There is no focus with $0 \leqq \mu_3 < \mu_2$. The same rules govern the whole subdomain A ($D_2 < 0$), of which $D_2 = 0$ appears as a fitting terminal. However, in B ($D_2 > 0$) foci begin to appear in pairs if $0 \leqq \mu_3 < \mu_2$, although there are still none if μ_3 is too small. This state of affairs persists through the entire B- and C-ranges and will be expected to be found with the value $D_2 = 1$ separating the two ranges.

Expression (7b) and (8) assume the forms

$$x_F = 2y_2 \sqrt{\frac{1 + K_2}{1 - K_2} \quad (D_3^2 - 1)}$$

$$\omega = \frac{1}{y_2^2} \left(\frac{D_3}{K_2 + 1}\right)^2 \quad \frac{\sqrt{q}}{(1 + q)^2} \quad .$$

* If μ_1 and μ_2 are both zero, $q = \frac{V_0}{\mu_3 y_2}$.

C. $D_2 = 1$

The gradient in the first layer is zero here, ($\mu_1 = 0$). Three essentially different classes of velocity profiles (Fig. 7) obey the necessary condition (3).

The limiting process $K_1 \to 1$ ($\mu_1 \to 0$, $\delta_1 \to 0$) transforms equation (6)

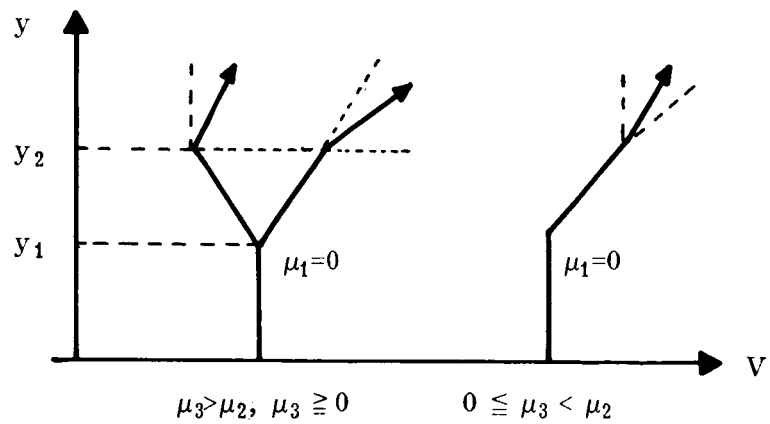

FIGURE 7. TYPICAL VELOCITY PROFILES WHEN $\mu_1 = 0$

into

$$v^3 + (\gamma - 1)\, v + \gamma \left(\frac{\mu_2}{\mu_3} - 1\right) = 0\,, \tag{33}$$

where

$$\gamma = (K_2 + 1)\, \frac{y_2 - y_1}{y_1}\,. \tag{34}$$

For the iteration of equation (33) one uses better the unknown

$$\varphi = v^3 = (1 + \delta_2 q)^{3/2} \tag{35}$$

writing

$$\varphi_{\nu+1} = (1 - \gamma)\, \varphi_{\nu}^{1/3} + \gamma \left(1 - \frac{\mu_2}{\mu_3}\right) \quad . \tag{36}$$

The two classes of profiles at the left of Figure 7 are specializations of the classes B and C in Figure 3. As these do, they give rise to one single source level focus out of the third layer. However, as with $\mu_2 = 0$, two iteration schemes must be set up to accommodate a coefficient in the equation, formerly $(D_3 - \beta)$, now $(1 - \gamma)$.

If the positive quantity γ remains less than unity, the process (36) converges monotonically. A suitable initial value was found as

$$\varphi_1 = 1 - \gamma \frac{\mu_2}{\mu_3} \quad . \tag{37}$$

which is always positive under the circumstances envisaged.

The rare event $\gamma = 1$ gives the direct solution

$$q = \operatorname{cotg}^2 \theta_0^* = \frac{\left(1 - \frac{\mu_2}{\mu_3}\right)^{2/3} - 1}{\delta_2} \quad .$$

With $\gamma > 1$ the reciprocal of φ, $t = \frac{1}{\varphi}$, sets equation (36) into the form

$$t_{\nu+1} = \frac{1}{\gamma\left(1 - \frac{\mu_2}{\mu_3}\right)} \left[1 + (\gamma - 1)\, t_{\nu}^{2/3}\right] \quad . \tag{38}$$

Monotonic convergence here is ensured; one may begin with

$$t_1 = \frac{1}{\left(1 - \frac{\mu_2}{\mu_3}\right)^3} \quad . \tag{39}$$

As was expected, the right profile type in Figure 7 ($0 \leqq \mu_3 < \mu_2$) does not always provide a third-layer focus. It is related to the B- and C-types of Figure 5. The critical quantity, there Q + R, here is

$$S = \left(\frac{1 - \gamma}{3}\right)^3 - \left[\frac{\gamma}{2}\left(\frac{\mu_2}{\mu_3} - 1\right)\right]^2 . \tag{40}$$

Focus formation is precluded if $\gamma \geqq 1$, or, more generally, if $S < 0$. It cannot take place with too small a value of μ_3.

The special case S = 0 yields the explicit solution

$$q = \frac{\frac{1 - \gamma}{3} - 1}{\delta_2} .$$

With $S > 0$, when of necessity $\gamma < 1$, two foci appear. One of them can be obtained after employing the approach (36) with the starting value (37). The other one follows from equation (33) when it is given the form

$$v_{\nu+1} = \frac{v_\nu^3 + \gamma\left(\frac{\mu_2}{\mu_3} - 1\right)}{1 - \gamma} . \tag{41}$$

The iteration may begin with

$$v_1 = \frac{\gamma}{1 - \gamma}\left(\frac{\mu_2}{\mu_3} - 1\right) \tag{42}$$

which is a positive quantity.

The expressions (7b) and (8) for x_F and ω must also be subjected to the limiting process $K_1 \rightarrow 1$. They then give

$$x_F = 2y_1 \sqrt{q}\left[\gamma + 2 + \delta_2 q\right]$$

$$\omega = \frac{1}{y_1^2} \frac{\sqrt{q}}{(1 + q)^2} \frac{1 + \delta_2 q}{[\gamma + 2 + \delta_2 q]\,[\gamma + 2 + 3\delta_2 q]} .$$

Use has been made here of equation (33) for simplification.

VII. A FOURTH SPECIAL TYPE: $V_2 = V_0$

The three classes of profiles occurring here mark the boundary of the classes C and D on Figures 3 and 5 (where the case $V_2 = V_0$, or $D_2 = \frac{y_2}{y_1}$ had been excluded). They are sketched in Figure 8.

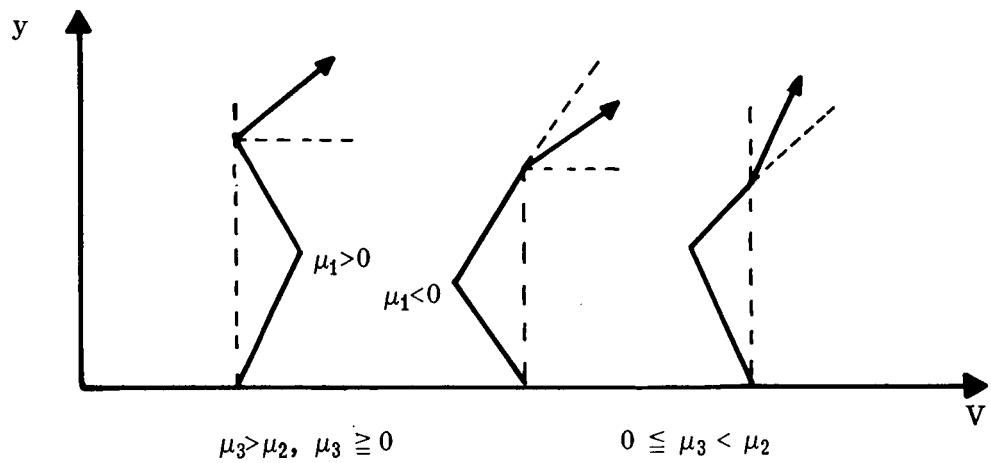

FIGURE 8. TYPICAL VELOCITY PROFILES WITH $K_2 = 1$

Since $K_2 = \frac{V_2}{V_0} = 1$, the inclination, θ_2, of a ray when entering the third layer* is equal to the inclination it had when leaving the sound source. With $\mu_1 > 0$, a group of small elevation rays is sent back to earth from the first layer and cannot enter the third. All those that do enter it will also return to source level, since the gradient μ_3 in the (infinitely extended) layer is not negative.

With $\delta_2 = 1 - K_2^2 = 0$ the u-equation (13), derived from the original focal equation (6), assumes the simple form

---

* θ_2 is given by $\sin \theta_2 = \sqrt{1 - K_2^2 \cos^2 \theta_0}$

$$u(1 + D_2 - D_3) = D_2 \quad . \tag{43}$$

If the parenthesis here is not negative, a positive solution for u exists. The condition may be written as

$$\frac{\mu_1}{\mu_3} + \frac{y_2}{y_1} \geqq 0. \tag{44a}$$

Since $\frac{\mu_1}{\mu_2} = 1 - \frac{y_2}{y_1}$, it is equivalent to the requirement

$$\frac{\mu_2}{\mu_3} \leqq \frac{y_2}{y_2 - y_1} \quad . \tag{44b}$$

With this relation upheld the solutions u of equation (43) can be shown to be physically relevant; i.e., they are larger or smaller than unity depending on whether $\delta_1 > 0$ or $\delta_1 < 0$* .

Since condition (44b) is fulfilled by the profiles belonging to the two left types on Figure 8 one single ground level focus will always develop with these as it will with any profile from the subdomains C and D in Figure 3.

The correspondence is not equally simple and complete when the third class of profiles is compared to the classes C and D on Figure 5. If μ_3 is too small (so that condition (44b) is violated), there will be no focus. An analogous behavior was found in the subdomain C; but in D, smallness of μ_3 does not prevent focus formation. On the other hand, if μ_3 is sufficiently large, one single focus will appear with $D_2 = \frac{y_2}{y_1}$, as it always will in subdomain D, while in C two foci will be generated by the third layer.

The expressions to be derived for θ_0^*, x_F, ω from equation (43) are relatively simple, and general results can be formulated as to the effects on them of μ_3 - variations. In the following the height y_2 and the entire velocity profile below it will be considered as parametrically fixed.

---

* With $\delta_1 = 0$, $V_1 = V_0 = V_2$, and $q = \frac{V_0}{\mu_3 y_2}$; see footnote on p. 26.

The quantity

$$\Delta = 1 - \frac{\mu_2}{\mu_3}\,\frac{y_2 - y_1}{y_2} = 1 + \frac{\mu_1}{\mu_3}\,\frac{y_1}{y_2} \tag{45}$$

is not negative, on the strength of conditions (44b) or (44a). Equation (42) can be solved for q to give

$$q = \operatorname{cotg}^2 \theta_0^* = \frac{1}{\delta_1}\left(\frac{1}{\Delta^2} - 1\right) . \tag{46}$$

One verifies without much labor that, in all three profile classes, a stronger third-layer gradient causes a steeper focal ray (θ_0^* increases).

Expression (7b) and (8) for the landing distance of the focal ray and for the intensity factor near the focus simplify to give

$$x_F = 2y_2\,(K_1 + 1)\,\sqrt{\frac{q}{1 + \delta_1 q}} \tag{47}$$

$$\omega = \frac{1}{[y_2\,(K_1 + 1)]^2}\left(\frac{1 + \delta_1 q}{1 + q}\right)^2 \sqrt{q} \quad . \tag{48}$$

For judging the dependence of these quantities on their argument q we consider the logarithmic differential quotients

$$\frac{1}{x_F}\,\frac{dx_F}{dq} = \frac{1}{2q(1 + \delta_1 q)} > 0 \tag{49}$$

$$\frac{1}{\omega}\,\frac{d\omega}{dq} = 2\,\frac{\delta_1 - 1}{(1 + \delta_1 q)\,(1 + q)} + \frac{1}{2q} . \tag{50}$$

This distance x_F decreases with q, i.e., with increasing angle of departure (θ_0^*). The steeper the focal ray, the nearer to the sound source it returns to ground level.

An equally unqualified statement cannot be obtained from the differential quotient (50) which can be positive, negative, or even zero. For the discussion we introduce ω from expression (48) and write

$$\frac{d\omega}{dq} = \frac{1}{[y_2 (K_1 + 1)]^2} \quad \frac{1 + \delta_1 q}{2\sqrt{q}\,(1 + q)^3} \quad [\delta_1 q (q + 5) + (1 - 3q)] \,. \qquad (50a)$$

The sign ambiguities in the last bracket are somewhat reduced by the restriction that cos θ_0^* must not be smaller than about 0.95 (see Introduction), or that

$$q \geqq \tilde{q} \approx 9 \,. \qquad (51)$$

The parenthesis (1 - 3q) is certainly negative then.

A few words may be intercalated here on the significance of the restriction (51) regarding other quantities in the case $V_2 = V_0$. First, although the landing distance decreases with q, it cannot decrease indefinitely without losing plausibility. To be sure, the focus would move into the sound source when $q = 0$, or $\theta_0^* = 90°$, but the supporting equations are then meaningless. Secondly, upper bounds are set up for the velocity gradients. From $u^2 \geqq 0$ it follows that

$$\mu_1 \leqq \frac{V_0}{y_1} \left(\sqrt{\frac{1 + \tilde{q}}{\tilde{q}}} - 1 \right) = 0.0541 \left(\frac{V_0}{y_1} \right) \,.$$

Furthermore, since $-\frac{\mu_2}{\mu_1} = \frac{y_1}{y_2 - y_1}$,

$$-\mu_2 \leqq 0.0541 \quad \frac{V_0}{y_2 - y_1} \,.$$

Finally, on combining expressions (46) and (45),

$$\mu_3 \leqq \mu_1 \frac{y_1}{y_2} \left[\frac{1}{\sqrt{1 + \delta_1 \tilde{q}}} - 1 \right]^{-1} \,.$$

Evidently, the restrictions on μ_1 and μ_2 are relevant with profiles of the first type only ($\mu_1 > 0$, $\mu_2 < 0$). The values of the three gradients encountered in practice rarely go beyond the above bounds, so that the restriction on θ_0^* seldom interferes with the interpretation of actual profiles.

Returning now to the discussion of ω let us first consider the left-hand class on Figure 8. Since $V_1 > V_0$ here, the quantity $\delta_1 = 1 - \left(\frac{V_1}{V_0}\right)^2$, and therefore the differential quotient (50a) is negative. The intensity parameter ω increases with θ_0^* : The larger μ_3, the steeper the focal ray, the closer the focus to the source, and the more serious is the focal situation. This is what might be called the regular sequence, also observed with the corresponding two-layer class arising when the middle layer is extended down to ground level.

As an example, consider the profile where $V_0 = V_2 = 340$ m/sec, $V_1 = 341$ m/sec, $y_1 = 100$ m, $y_2 = 200$ m. The upper bounds for μ_1 and $-\mu_2$ are both $0.184 \frac{1}{\text{sec}}$, while, in fact, $\mu_1 = -\mu_2 = 0.01 \frac{1}{\text{sec}}$, well below the ceiling. Since $\delta_1 \approx -\frac{1}{170}$, the upper bound on μ_3 in $\approx 0.188 \frac{1}{\text{sec}}$. With

$$\mu_3 = 0.02 : \Delta = 1.25, \quad q = 61.2, \quad \theta_0^* = 7°17', \quad x_F = 7.84 \text{ km}$$

$$\mu_3 = 0.04 : \Delta = 1.125, \quad q = 35.7, \quad \theta_0^* = 9°30', \quad x_F = 5.39 \text{ km}.$$

When the focus moves from the first to the second position the average intensity near it increases by the factor $\frac{\omega_2}{\omega_1} = 3.33$, or by 5.2 db.

Profiles with $\mu_1 > 0$ confine low elevation rays to the ground layer. The first ray that can possibly escape it is characterized by $\sqrt{1 - K_1^2 \cos^2 \theta_0} = 0$, or by $\text{cotg}^2 \theta_0 = -\frac{1}{\delta_1}$. The gradient in the second layer being negative, that ray will traverse it and enter the third layer under the angle $\theta = \theta_0$. It will be a focal ray ($\theta_0 = \theta_0^*$) if $q = -\frac{1}{\delta_1}$ satisfies the focal equation (46), i.e., if $\Delta = \infty$ and, therefore, $\mu_3 = 0$. Because it has the lowest angle of departure of all the focal rays, it will be returned farther out and with lower intensity than any other ray. Indeed, by expression (47) and (48), $x_F = \infty$ and $\omega = 0$. This clearly is a mathematical result devoid of practical significance.

With the two right-hand classes in Figure 8 (where $\mu_1 < 0$, $\delta_1 > 0$), the ground layer cannot restrain any ray from going up and penetrating into the second layer. On the other hand, even a mathematical focal situation cannot develop if $\mu_3 = 0$. By condition (44b), the smallest value of μ_3 that still permits focus formation out of the third layer is given by

$$\frac{\mu_2}{\mu_3} = \frac{y_2}{y_2 - y_1} > 1 \ .$$

It defines a profile of the third class for which the zero-ray is focal ray, since $\Delta = 0$, $q = \infty$, $\theta_0^* = 0$. This ray culminates at the boundary of the second and third layers and, by expressions (47) and (48), is returned at the (largest possible) distance

$$x_F = 2y_2 \sqrt{\frac{1 + K_1}{1 - K_1}}$$

with the intensity parameter

$$\omega = \infty \ .$$

A very strong focus can be expected here. In passing, it will be observed that, if x_F and $\left.\frac{d^2x_s}{d\theta_0^2}\right|_{\theta_0 = \theta_0^*}$ remain finite, the general expression (7) shows that the intensity factor will always exceed all bounds if θ_0^* can and does approach zero. High noise levels at rather large distances may sometimes be explainable that way.

On increasing μ_3 the focal distance will decrease; the intensity factor, contrary to its usual behavior, cannot but decrease, too, and does so at a fast pace, since the cotangent-function drops rapidly when its argument increases from zero on. This trend continues down to a minimum of ω which, by expression (50a), can be determined after solving the quadratic

$$\delta_1 q^2 + (5\,\delta_1 - 3)\ q + 1 = 0$$

Since the positive quantity δ_1 is very small the solutions may be given as

$$q \approx \frac{3 - 5\delta_1}{2\delta_1}\left[1 \pm \left(1 - \frac{2\delta_1}{(3 - 5\delta_1)^2}\right)\right] ,$$

or, more explicitly, as

$$q \approx \frac{3 - 5\delta_1}{\delta_1} \quad \text{and} \quad q \approx \frac{1}{3 - 5\delta_1} .$$

Of these, the second solution is too small and must be disregarded. The values of ω and Δ related to the first are found as

$$\omega_m \approx \frac{1}{[y_2 (K_1 + 1)]} \left[\frac{4}{9}\sqrt{3}\ \delta_1^{3/2}\right]$$

$$\Delta_m \approx \frac{2}{4 - 5\delta_1} \approx \frac{1}{2} .$$

Rearranging relation (45) to give

$$\frac{\mu_3}{\mu_2} = \frac{1}{1 - \Delta} \frac{y_2 - y_1}{y_2} ,$$

we see that enlarging μ_3 results in larger values of Δ, and therefore of θ_0^*. When μ_3 has grown to equal μ_2, the dividing line between the two right-hand classes in Figure 8 has been reached, characterized by $\Delta = \frac{y_1}{y_2}$. If this value is still smaller than Δ_m, i.e., if $y_2 > 2y_1$, the intensity factor ω is still decreasing; if $y_2 < 2y_1$, it will have passed its minimum and increase. Conceivably, the second layer's thickness, $(y_2 - y_1)$, could be so large that no realistic value of μ_3 will suffice to carry ω beyond the minimum. However, in ordinary circumstances values

$$\mu_3 > 2\mu_2 \frac{y_2 - y_1}{y_2}$$

can be admitted. With such profiles the "regular" sequence obtains: ω becomes stronger with μ_3.

Take, for instance,

$$V_0 = V_2 = 340 \text{ m/sec}, \; V_1 = 339.32 \text{ m/sec}, \; y_1 = 50 \text{ m}, \; y_2 = 200 \text{ m} .$$

Figure 9 is based on these data. The focus abscissa, x_F, has been taken as the independent variable instead of μ_3. The ration $\frac{\mu_3}{\mu_2}$ and the intensity level are plotted versus x_F.

The second layer velocity gradient is the constant

$$\mu_2 = -\frac{1}{3}\mu_1 \quad , \quad \mu_1 = -0.0136 \; .$$

The average intensity level near a focus,

$$IL = 10 \log_{10} \frac{\omega}{\omega^*} \quad ,$$

contains the arbitrary reference value ω^*. In Figure 9, ω^* has been left undetermined, so that no absolute values are given on the db-scale.

The foci at the left of $x_F \approx 12.2$ km ($\mu_3 = \mu_2$) are created by profiles belonging to the middle class in Figure 8. It is seen that, if $\frac{\mu_3}{\mu_2} \approx 1.5$, the focus will reside at $x_F \approx 11$ km, and the average intensity near it will be least alarming. It will, however, increase irrespective of whether μ_3 is increased or decreased. The "regular" (two-layer) sequence prevails at the left of the minimum. The curves are terminated at $x_F = 5$ km, corresponding to $\mu_3 = 0.0425$ (a value that seldom will be exceeded*). The focal ray existing with this

---

* The sound propagation velocity would then increase by 4.25 m/sec for every 100 m up in the third layer.

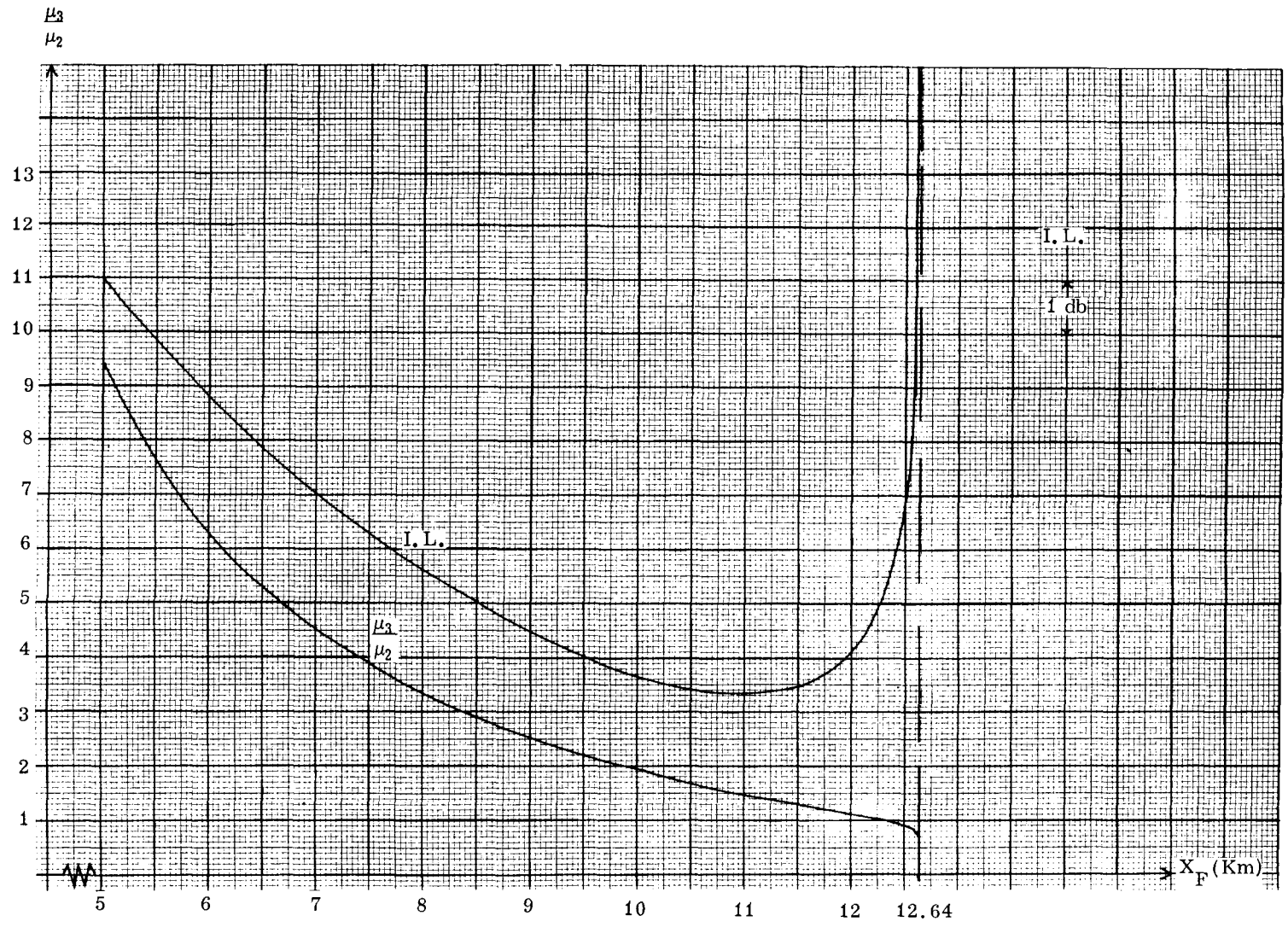

FIGURE 9. GRADIENT RATIO REQUIRED TO LOCATE THE FOCUS AT x_F AND AVERAGE INTENSITY LEVEL THERE. $K_2 = 1$.

particular profile has the initial elevation $\theta_0^* = 8°20'$. The maximum elevation, θ_1^*, is given by $\sin \theta_1^* = \sqrt{1 - K_1^2 \cos^2 \theta_0^*}$; since $K_1 = \frac{V_1}{V_0}$ is but little different from unity, the angle θ_1^* is insignificantly larger than θ_0^* and well within the range of validity for the θ.

The foci at the right of $x_F \approx 12.2$ km exist with third-class profiles (Fig. 8). If the middle layer were extended to ground level, the corresponding two-layer atmosphere thus obtained could not support a focus at all. On decreasing μ_3, the average intensity level grows very rapidly, and small differences in μ_3 (and x_F) will affect it out of proportion. The focal rays here are all of very small initial elevation, the zero-ray ($\theta_0^* = 0$) arriving at the (largest possible) distance $x_F = 12.64$ km, corresponding to $\frac{\mu_3}{\mu_2} = \frac{y_2 - y_1}{y_2} = 0.75$ and $\omega = \infty$. If μ_3 is decreased still further, a focal situation in the usual sense cannot develop. However, ray tubes of very small initial elevation will, whatever the positive gradient μ_3 might be, always arrive near $x = 12.64$ km and enclose a very small frontal area causing a focus-like high intensity level. This is a general result: With profiles capable of returning the zero ray at a finite distance high levels will always be found there, although, in general, $\theta_0 = 0$ will not solve the focal equation. Machine computations in such cases show declining intensity with increasing small θ_0-values; however, since the first value is usually $\theta_0 = 0.2°$, they do not exhibit the very large intensities to be expected if θ_0 is even smaller.

VIII. CONCLUSION

The three-layer "planar" atmospheres can be classified with the use of the parameter

$$D_2 = 1 - \frac{\mu_1}{\mu_2},$$

where the constant quantity μ_k denotes the sound speed variation per unit length climb in the k^{th} layer.

Acoustical foci on the ground may develop if μ_3 is positive. Adapted to the various atmospheric classes, computational schemes can be set up for finding the focus location and the average noise level in its immediate neighborhood.

If $\mu_3 > \mu_2$ one single focus will appear (provided the third layer is extended enough to turn around the focal ray). An analogous statement holds in a two-layered atmosphere with $\mu_2 > 0$ and $\mu_2 > \mu_1$. Even if $\mu_3 < 0$, a second-layer focus can develop in those circumstances.

In the realm $0 < \mu_3 < \mu_2$ the existence criteria are less clear-cut. There can always be a third-layer focus if $D_2 > \frac{y_2}{y_1}$. For smaller values of D_2, the value of μ_3 must attain a certain minimum before foci can appear; but then as many as two may develop with a given meteorology. These occurrences have no counterpart in the two-layered atmosphere where the equivalent condition $0 < \mu_2 < \mu_1$ does not permit any focus formation.

A second-layer focus will move toward the sound source and the average intensity level near it will rise if at a given value of μ_1 the value of μ_2 is increased. A third-layer focus does not always respond in the same manner to a variation of μ_3 at fixed values of μ_1 and μ_2. It may draw nearer to the sound source with diminishing intensity level.

Systematic surveys of the behavior of third-layer foci are planned. These will be carried out with the relatively easy methods described in the present report.

LIST OF REFERENCES

1. Rothwell, P.: Calculation of Sound Rays in the Atmosphere. Journal Acoustic Society of America, vol. 19, no. 1, Jan. 1947.

2. Blumke, C.; et al.: Feasibility Study of an Aerocap Supported Meteorological Measuring System. The Electronics Division of General Mills, Inc., Sept. 1961.

3. Mabry, James E.: Dependence of the Acoustical Focus Location on Meteorological Conditions in the Two-Layered Atmosphere. MTP-AERO-62-60.

4. Heybey, W.: Notes on Sound Propagation and Focusing. MTP-AERO-62-17.

GROUND LEVEL ACOUSTICAL FOCI IN A THREE-LAYERED ATMOSPHERE

By Willi H. Heybey

The information in this report has been reviewed for security classification. Review of any information concerning Department of Defense or Atomic Energy Commission programs has been made by the MSFC Security Classification Officer. This report, in its entirety, has been determined to be unclassified.

This report has also been reviewed and approved for technical accuracy.

W. H. Heybey

W. H. HEYBEY
Aero-Astrodynamics Laboratory, T

E. D. GEISSLER
Director, Aero-Astrodynamics Laboratory

DISTRIBUTION

INTERNAL

DIR
AST-S
DEP-T
MS-IP
MS-IPL (8)
R-AERO
Dr. Geissler
Mr. Jean
Mr. Reed
Mr. Wilhold
Mr. Murphree
Dr. Heybey (20)
Dr. Sperling
Mr. Cummings
Mr. Dickey
Mr. Mabry
Mr. Peasley
Mr. Vaughan
Mr. Turner
Mr. Scoggins
Mr. O. Smith (5)
Mr. Baker
Mr. Lindberg
Mr. Dahm
Mr. Holderer
Mr. Linsley
Dr. Krause
Mr. Horn
Mr. Lavender
Mr. Rheinfurth
Mr. Jess Jones
R-ASTR
Dr. Haeussermann
Mr. Hoberg
Mr. Bell
CC-P
MS-T (5)
Mr. R. Bland
R-COMP
Dr. Hoelzer
Mr. Harness
Dr. Polstorff
I-E
Mr. Belew
Mr. Morea
E-DIR
I-DIR
Col. O'Conner
Dr. Hueter
Dr. Mrazek
I-MICH
Mr. Constan
R-P&VE
Mr. Cline
Mr. Hellebrand
Mr. Burrows
Mr. Showers
Mr. Farrow
Mr. Gassaway
Mr. Johnston
R-QUAL
Mr. Grau
Mr. Schulze
R-DIR
Mr. Weidner
Dr. McCall
MS-H
HME-P
R-ME
Mr. Kuers
MTF
Mr. Fortune
Mr. Nybo (2)
Mr. Antler
I-RM-M

INTERNAL (Cont'd)

KSC
Mr. Gorman
Dr. Knothe
Mr. Poppel
Mr. Brewster
Mr. Hershey
Mr. Wilkinson
Dr. Bruns
Major Petrone
Mr. Dodd
Mr. Sendler
Mr. Gruene
Mr. Zeiler

R-RP
Dr. Stuhlinger

R-TEST
Mr. Heimburg
Dr. Sieber
Dr. Reisig (2)
Mr. Rutledge
Mr. McBryde

PAO
Mr. Slattery

R-SA
Mr. Dannenberg

I-I/B
Mr. James

EXTERNAL

AMSMI-RRA
Dr. Essenwanger

Research Institute
University of Alabama Extension Center
Attn: Dr. R. Hermann

ORDXM-OTL
Technical Library, AMC (5)

Jet Propulsion Laboratory,
CCMTA
H. Levey

Dr. C. E. Buell
Karman Nuclear
Garden of the Gods Road
Colorado Springs, Colo.

NASA Headquarters
OART, Code RD-1
Attn. Mr. Fred J. Demerritte
Mr. Greene

NASA Headquarters
OART, Code RDA
Attn: Mr. Underwood

NASA Headquarters
OMSF, Code MTC
Attn: Mr. W. Bos

NASA Headquarters
OSSA, Code SFM
Attn: Mr. Spreen

NASA Headquarters
OSSA, Code SV
Attn: Mr. Hamby

Director,
Office of Manned Space Flight (3)
NASA
Washington 25, D. C.

EXTERNAL (Cont'd)

Langley Research Center
NASA
Langley Field, Hampton, Virginia
Director (2)
Mr. Hubard, Chief, Acoustics Br.

Director, Goddard Space Flight Center (2)
Greenbelt, Maryland

Director, Ames Research Center (2)
NASA
Moffett Field, California

Lewis Research Center
NASA
2100 Brookpark Road
Cleveland 35, Ohio
Director (2)
Technical Information Division (2)

Engineer in Charge (2)
Wallops Station
National Aeronautics and Space Administration

Director, Manned Spacecraft Center (2)
Post Office Box 1537
Houston, Texas

Pacific Missile Range (2)
Technical Library

White Sands Proving Ground
Technical Library
US Army ER & DA (2)

Commander, AF Missile Test Center
Patrick AFB, Fla.,
Attn: Technical Information & Intelligence Office MIGRY

EXTERNAL (Concluded)

Hq. 6570 Aero Space Medical Research
Aero Space Division, AFSC
Wright Patterson AFB
Dayton, Ohio
Von Gierke (2)
Cole (2)

Scientific and Technical Information Facility (25)
Attn: NASA Representative (S-AK/RKT)
P. O. Box 33
College Park, Maryland 20740

Commanding Officer
U. S. Army Electronics and Development Activity
White Sands Missile Range
New Mexico
Attn: SELWS-M

Martin-Marietta Corp.
P. O. Box 179
Denver 1, Colorado
Attn: C. R. Gunnison, A-175